Hydrol. Earth Syst. Sci., 15, 295–310, 2011
www.hydrol-earth-syst-sci.net/15/295/2011/
doi:10.5194/hess-15-295-2011

Hydrology and Earth System Sciences

Particular uncertainties encountered in using a pre-packaged SEBS model to derive evapotranspiration in a heterogeneous study area in South Africa

L. A. Gibson[1,2], **Z. Münch**[3], **and J. Engelbrecht**[4]

[1]Agricultural Research Council-Institute for Soil, Climate and Water, Private Bag X5017, Stellenbosch, 7599, South Africa
[2]Department of Environmental and Geographical Science, University of Cape Town, Shell Environmental & Geographical Science Building, South Lane, Upper Campus, University of Cape Town, Private Bag X3, Rondebosch 7701, South Africa
[3]Stellenbosch University, Private Bag X1, Matieland, 7602, South Africa
[4]Council for Geoscience, Western Cape Unit, P.O. Box 572, Bellville, 7535, South Africa

Received: 23 July 2010 – Published in Hydrol. Earth Syst. Sci. Discuss.: 1 September 2010
Revised: 22 December 2010 – Accepted: 12 January 2011 – Published: 25 January 2011

Abstract. The focus of this paper is on the pre-packaged version of SEBS in ILWIS and the sensitivity of SEBS to some parameters over which the user has some control when using this version of the model, in order to make informed choices to limit uncertainties. The sensitivities of SEBS to input parameters are related to daily ET rather than energy flux results since this is of interest to water managers and other users of the results of the SEBS model. This paper describes some of the uncertainties introduced by the sensitivity of the SEBS model to (a) land surface temperature and air temperature gradient, (b) the choice of fractional vegetation formula, (c) displacement height and the height at which wind speed is measured, and (d) study area heterogeneity. It was shown that SEBS is sensitive to land surface temperature and air temperature gradient and the magnitude of this sensitivity depended on the land cover and whether or not the wet-limit had been reached. The choice of fractional vegetation cover formula was shown to influence the daily ET results by up to 0.7 mm. It was shown that the height of the vegetation canopy should be considered in relation to the weather station reference height to avoid the sensible heat flux from becoming unsolvable due to a negative ln calculation. Finally the study area was shown to be heterogeneous although the resolution at which fluxes were calculated did not significantly impact on energy partitioning results. The differences in the upscaling from evaporative fraction to daily ET at varying resolutions observed implies that the heterogeneity may play the biggest role in the upscaling and the influence of albedo on this calculation should be studied.

Correspondence to: L. A. Gibson
(gibsonl@arc.agric.za)

1 Introduction

The pressure on water resources in South Africa creates a need for water resource managers to have accurate information on all aspects of water resource occurrence and use. To quantify the various components involved in calculating water use by means of field-based observations would be a difficult and time consuming process, providing only point-based measurements at a specific point in time. This problem is compounded when one considers that several measurements over time would be needed to accurately measure or monitor water use. To address these problems, Gibson et al. (2010) investigated the usefulness and applicability of remote sensing technologies as a tool for water resource assessment and specifically for the quantification of water use at farm level. Their approach relied on a simplified equation in which each component of the water balance equation was calculated for a hydrological year using mostly remote sensing techniques or products where possible.

To derive the remote sensing datasets for input into water balance equations, several complex models were applied to the input data. Although all of the components quantified by remote sensing data were subject to uncertainties and limitations, Gibson et al. (2010) were alerted to the possibility of uncertainties through the calculation of evapotranspiration (ET). The calculation of ET revealed that the total annual ET ($1.397\,km^{-3}$) calculated using the Surface Energy Balance System (SEBS) model for the study area exceeded the total rainfall ($0.771\,km^{-3}$) for the same area and time period. Although it may be possible for annual actual evapotranspiration to exceed annual precipitation in certain instances, such as where large scale irrigation from groundwater resources is practiced, in this particular study, it is believed that actual

Published by Copernicus Publications on behalf of the European Geosciences Union.

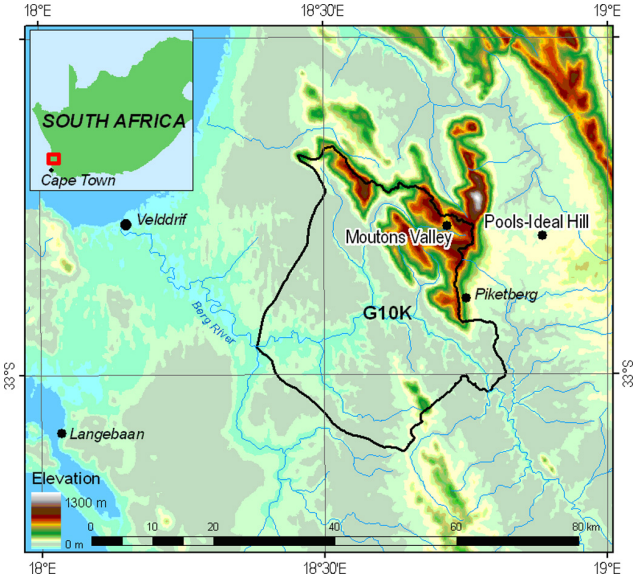

Fig. 1. Orientation map showing the G10K catchment, the Mouton's Valley field validation site and the weather station Piketberg: Pools-Ideal Hill (shown as Pools-Ideal Hill) situated in a dryland agricultural area which was used for experimental purposes.

evapotranspiration was overestimated. Since irrigated agriculture forms a small portion of the catchment (2.4%) in comparison to natural vegetation (29.7%) and dryland agricultural (66.5%), the higher actual evapotranspiration than precipitation at catchment scale cannot be ascribed to evaporative losses due to irrigation. As a consequence, the origins of uncertainties with regard to the accuracy of the final results were explored using the estimation of ET as an example.

The derivation of ET is a complex process requiring several sources of input data and numerous processing steps to derive intermediate output products. The intermediate products are then combined through additional processing algorithms to derive the final daily ET product. The SEBS model is available as part of the open source freeware ILWIS (available at www.52north.org), therefore it can be used by practitioners with remote sensing knowledge who may not necessarily have the micrometeorological expertise to develop a model themselves to estimate ET. Whilst the open-source format of SEBS is very useful and can speed up the research process, there are some instances where specialist knowledge is required to implement the model correctly to derive the most accurate results. Furthermore, the complexity of the SEBS model together with the inherent uncertainty in using remote sensing derived products as input implies that a large number of sources of uncertainty may exist and should be properly understood.

This paper attempts to highlight some of the uncertainties encountered when using the SEBS model in a heterogeneous area in South Africa. Several authors have addressed issues related to sensitivity of the SEBS model to various input parameters (most notably van der Kwast et al., 2009). This paper differs in that it focuses on the pre-packaged version of SEBS in ILWIS and the sensitivity of SEBS to some parameters over which the user has some control when using this version of the model, so informed choices can be made at various stages in the processing chain, in order to limit the introduction of unnecessary uncertainties. Furthermore, in this paper the sensitivities of SEBS to input parameters is related to daily ET rather than energy flux results since this is of interest to water managers and other users of the results of the SEBS model. This paper will describe some of the uncertainties introduced by sensitivity of the SEBS model to (a) land surface temperature and air temperature gradient, (b) the choice of fractional vegetation formula, (c) displacement height and the height at which wind speed is measured, and (d) study area heterogeneity.

2 Study area

The study area, situated in the Piketberg region in the Western Cape Province of South Africa (Fig. 1), encompasses a quaternary catchment (G10K) in which commercial agriculture plays an important role. The area experiences winter rainfall (May to October), has a diverse topography and is drained by the perennial Berg River which enters the Atlantic Ocean at Velddrif on the West Coast.

The climate in the area is varied with the western part of the catchment experiencing a maritime Mediterranean climate whilst the eastern part is considered to have a continental influence. The varying climate has an influence on the land use in the area with low-lying areas being dominated by dryland agriculture (predominantly wheat fields). In addition, temporary commercial irrigated agriculture (potatoes) under centre pivot irrigation as well as pockets of natural vegetation, described as shrublands and low fynbos, are found. The elevated area towards the northeast of the catchment is dominated by natural vegetation in the form of low- and high-fynbos with reported alien vegetation infestations. Cultivated irrigated lands in the form of deciduous and citrus fruit tree orchards are also found, although to a lesser extent.

Energy balance and evapotranspiration field measurements by Jarmain and Mengistu (2009) in an apple orchard on Moutons Valley farm from 7 November to 1 December 2008 were used to validate the results obtained by Gibson et al. (2010). Jarmain and Mengistu (2009) used a one-sensor Eddy covariance system for the estimation of the sensible heat flux density. The instrumentation was installed in the middle of the apple orchard in a section planted with Royal Gala trees. An RM Young three-dimensional ultrasonic anemometer (model 81000, Traverse city, Michigan, USA – path length of 150 mm) was used to estimate sensible heat flux density. Two net radiometers were used to measure the net radiation above the apple orchard. One REBS Q*6 net radiometer was installed above the apple tree row,

and one NR-Lite net radiometer (Model 240-110, Kipp and Zonen) was installed above the inter-row area. The average value of these two sensors was used in the calculations. Soil temperature (using type-E soil averaging thermocouples) and soil heat fluxes (REBS heat flux plates) were measured at four different positions between the tree rows and the data was used to estimate the soil heat flux density. Using the estimates of sensible heat flux density and that of net irradiance and soil heat flux density, the latent energy flux density was subsequently calculated using the shortened energy balance equation (Jarmain and Mengistu, 2009).

At the time of the energy balance and total evaporation measurements in November 2008, the average canopy height was 3.2 m. The apple trees did not cover the soil surface completely, rather by about 75% and the inter-row areas were planted with grass (Jarmain and Mengistu, 2009).

Due to limited financial resources, field validation could not be conducted at multiple sites or for the entire hydrological year for which the water balance components were calculated. Therefore energy flux results presented in this research correspond to the specific field validation site (hereafter referred to as Mouton's Valley site) and period. In addition, an automatic weather station installed in a dryland agricultural area (hereafter referred to as Piketberg: Pools-Ideal Hill site) was used to compare results between land covers. However, there was no validation data available for this site.

3 Materials and methods

The Surface Energy Balance System (SEBS) is a model proposed by Su (2002) for the estimation of atmospheric turbulent fluxes and evaporative fraction using satellite earth observation data in combination with meteorological information. The SEBS model is used to estimate daily actual ET from remotely sensed and meteorological data by calculating the energy required for water to change phase from liquid to gas:

$$\lambda E = R_n - G_0 - H \tag{1}$$

where λE is the turbulent latent heat flux (λ is the latent heat of vaporization and E is water vapour flux density), R_n is net radiation, G_0 is the soil heat flux and H is the sensible heat flux (Su, 2002). The complete formulation of the SEBS model is given by Su (2002).

Reflectance and radiance measured by space-borne sensors are used to calculate land surface parameters – albedo, emissivity, land surface temperature, NDVI and fractional vegetation cover. The meteorological inputs required are radiation[1] ($W\,m^{-2}$), temperature[1,2] (°C), air pressure[1] (Pa) at surface and at reference height, specific humidity[1] ($kg\,kg^{-1}$) wind speed[1] ($m\,s^{-1}$) at reference height and sunshine duration[2] (hours). Instantaneous values are used in the calculation of the evaporative fraction and daily values are used for the upscaling of the evaporative fraction to daily ET. A simplified sequence illustrating the processing in SEBS is given in Table 1.

According to Su (2006), it is possible to estimate the latent heat flux as a residual after the sensible heat flux has been derived. However, because the sensible heat flux is not constrained by the available energy but is determined solely by surface temperature and the meteorological conditions at the reference height, there is an associated uncertainty in the derived latent heat flux and therefore also in the evaporative fraction. However, in SEBS this uncertainty is limited by considering the energy balance at the limiting cases since the actual sensible heat flux is constrained to the range set by the sensible heat flux at the wet limit (derived from a combination equation), and the sensible heat flux at the dry limit (set by the available energy).

According to formulations by Su (2002), the relative evaporation is derived from the sensible heat flux and the sensible heat flux calculated at the wet and dry limits. The relative evaporation is, in turn, used together with R_n, G_0 and the latent heat flux at the wet limit to estimate the evaporative fraction (Eqs. 2 and 3).

$$\Lambda_r = 1 - \frac{H - H_{wet}}{H_{dry} - H_{wet}} \tag{2}$$

Where Λ_r is relative evaporation, H is the sensible heat flux and H_{wet} and H_{dry} are the sensible heat flux at the wet and dry limits respectively.

$$\Lambda = \frac{\lambda E}{R_n - G_0} = \frac{\Lambda_r \cdot \lambda E_{wet}}{R_n - G_0} \tag{3}$$

Where Λ is the evaporative fraction and λE and λE_{wet} are the latent heat flux and the latent heat flux at the wet limit, respectively.

In SEBS it is assumed that the daily value of evaporative fraction is approximately equal to the instantaneous value, and from this, the daily evaporation can be determined as

$$ET = 8.64 \times 10^7 \times \frac{\Lambda \cdot \overline{R_n}}{\lambda \rho_w} \tag{4}$$

where ET is the actual evaporation on daily basis ($mm\,d^{-1}$), λ is the latent heat of vaporization ($J\,kg^{-1}$), ρ_w is the density of water ($kg\,m^{-3}$) and $\overline{R_n}$ is the daily net radiation flux (Lin et al., 2008).

The daily net radiation flux is given as:

$$\overline{R_n} = (1 - c_1) \cdot r_o \cdot K\downarrow_{day} + L_{day} \tag{5}$$

where c_1 is a conversion factor of 1.1 for instantaneous to broad band albedo, r_o is broad band albedo as calculated from the formulae by Liang (2000) and used in the instantaneous net radiation flux calculation in SEBS (see Table 1), $K\downarrow_{day}$ is incoming shortwave radiation (measured or modeled) and L_{day} is daily longwave radiation (Hailegiorgis,

[1] Instantaneous, i.e. hourly average at time of satellite overpass

[2] Daily average

Table 1. Sequence of SEBS processing (adapted from Su et al., 2008).

Inputs		Outputs
Incoming shortwave radiation (SW↓), land surface temperature (θ_0), albedo (α), air temperature (θ_a), land surface emissivity (εa)	→	Net radiation (R_n)
Fractional vegetation cover (fc), α, R_n	→	Land surface emissivity (εa), Soil heat flux (G_0) Sensible heat flux (H_{dry})
R_n, G_0	→	Sensible heat at the dry limit (H_{dry})
Horizontal wind speed (U), T_0, T_a, Leaf Area Index (LAI), Roughness length for momentum transfer (Z_{0m}), fc	→	Frictional velocity (u*), Monin-Obukhov length (L), Sensible heat flux (H), Excess resistance to heat transfer (kB^{-1}), Roughness length for heat transfer (Z_{0h})
Specific humidity (es), R_n, G_0, u*, Z_{0h}	→	Wet-limit stability length (L_{wet}), Sensible heat flux at the wet limit (H_{wet})
H_{dry}, H_{wet}, H	→	Relative evaporation (Λr)
H_{wet}, R_n, G_0	→	Evaporation at the wet limit (λE_{wet})
λE_{wet}, Λr , R_n, G_0	→	Evaporative fraction (Λ)
Λ, Daily radiation (R_{n24}), Daily soil heat flux (G_{24})	→	E_{daily}

2006). It can be seen from Eqs. (4) and (5) that aside from evaporative fraction itself, albedo is the sole remote sensing derived variable used in the upscaling from instantaneous evaporative to daily ET.

Published results of the SEBS model have been validated with a variety of field and/or complementary methodologies such as the extremely localised lysimeter (Lin, 2006), flux tower measurements using Eddy covariance or Bowen Ration methods (Su, 2002; Su et al., 2005; Timmermans et al., 2005; McCabe and Wood, 2006; Badola, 2009; van der Kwast et al., 2009), the large aperture scintillometer (Jia et al., 2003; Timmermans et al., 2005). Additionally, results have been compared to hydrometeorological equations (Hailegiorgis, 2006; Lin, 2006; Gebreyesus, 2009) and the water balance or by examining hydrological consistency with other datasets (Su and Roerink, 2004; Alvarez, 2007; McCabe et al., 2008; Pan et al., 2008).

For the purpose of calculating ET in this research, MODIS TERRA and AQUA data (MOD021KM _ Level 1B Calibrated Radiances – 1 km: Collection 5) were used. MODIS images are captured daily or every second day and therefore it is possible, in South Africa, to obtain a good coverage throughout the year. MOD02 and MYD02 data were selected for the field validation period. Single date (28 February 2008) ASTER level 1B – Registered Radiance at the Sensor, and ASTER level 2 – AST08 Surface Kinetic Temperature, were used to compare the results of the higher resolution sensor to those of the same date coarser resolution MODIS sensor. The required meteorological data (air temperature, wind speed, radiation, sunshine duration) can be obtained directly from an automatic weather station (AWS) or indirectly (air pressure, specific humidity) using empirical formulae and data from the AWS. Weather data from the Mouton's Valley and the ARC-ISCW, Piketberg: Pools-Ideal Hill AWSs were used.

4 Uncertainties in evapotranspiration estimates with SEBS

The analysis of remote sensing and GIS products usually results in maps of discrete or continuous variables (Dungan et al., 2002), which can be associated with several sources of error or uncertainty. These include: (1) errors or uncertainties associated with the specific remote sensing data obtained; (2) errors or uncertainties introduced with the processing and analysis of image and field data; (3) errors or uncertainties associated with the specific model; and (4) errors or uncertainties associated with positional aspects (including image resolution). Wang et al. (2005) identify additional sources of errors including sampling and measurement error of ground truth data, errors of spectral values and radiometric calibration of images, errors from the leap from spectral measurements to interpretation of a categorical variable, modelling errors due to misunderstanding the relationship between spectral and thematic variables, and errors from GIS operations.

Several authors have addressed the sensitivity of the SEBS model to various input parameters including: roughness length (Lin, 2006; Alvarez, 2007; van der Kwast et al.,

2009; Gebreyesus, 2009), displacement height (Lin, 2006), land surface temperature (Badola, 2009; van der Kwast et al., 2009), wind speed and wind direction (van der Kwast et al., 2009), fractional vegetation cover (Badola, 2009; Lin, 2006), surface emissivity (Badola, 2009; van der Kwast et al., 2009; Lin, 2006), albedo (Badola, 2009; van der Kwast et al., 2009), NDVI (Badola, 2009; van der Kwast et al., 2009), shortwave incoming radiation (van der Kwast et al., 2009) and the height of the planetary boundary layer (van der Kwast et al., 2009).

In the formulation publication of SEBS (Su, 2002), the sensitivity of the sensible heat flux to parameters used in it's calculation (land surface temperature and air temperature gradient, friction velocity, excess resistance to heat transfer, and stability correction function for heat transfer) was found to be around 40 $W\,m^{-2}$ when the various terms are assumed independent of each other. Since in reality, at least some of the terms are correlated, the expected sensitivity can then be estimated in the order of 20 ($W\,m^{-2}$), which is around 20% relative to the mean sensible heat flux (H) (Su, 2002). Of the reported sensitivities since the work of Su (2002), Badola (2009) and van der Kwast et al. (2009) reported SEBS to be most sensitive to land surface temperature. However, Lin (2006) reported that the SEBS model is most sensitive to roughness length and according to van der Kwast et al. (2009), sensitivity to aerodynamic parameters (roughness length, displacement height and canopy height) and the method used to derive these parameters should be considered depending on the heterogeneity of the image footprint.

Uncertainties in the derivation of ET for this study were identified as (but are by no means limited to): (1) land surface and air temperature gradient; (2) the choice of fractional vegetation cover formula; (3) displacement height and the height of wind speed measurement in relation to displacement height; and (4) study area heterogeneity.

4.1 Land surface and air temperature gradient

The calculation of ET using the SEBS model relies on two temperature sources: air temperature (T_a) and land surface temperature (T_0). Su (2002) reported on the sensitivity of sensible heat flux to the gradient between land surface temperature and air temperature hourly and Badola (2009) reported that of all remotely sensed input parameters, SEBS was most sensitive to change in $(T_0 - T_a)$. T_0 plays a role in the determination of net radiation (R_n) (Table 1) and therefore soil heat flux (G_0), but its main contribution (together with the aerodynamic resistance) is in the calculation of the sensible heat flux.

To quantify the uncertainty associated with T_0 estimates for the field validation site, the T_0 retrieved from MODIS data was compared with the Meteosat SEVIRI T_0 data product (SEVIRI/Meteosat LST Product: LSA-4 (MLST) Product version 7.2) corresponding to the same time of image acquisition. The motivation for using Meteosat SEVIRI T_0 data was to try to set a realistic uncertainty range in T_0 in this particular heterogeneous environment. It was found that there were differences of up to 10 K between MODIS T_0 and SEVIRI T_0 with SEVIRI T_0 being consistently higher than MODIS T_0 which is in agreement with the findings by Madeira et al. (2005). This high degree of uncertainty in T_0 can be ascribed to the topographically rough nature of the terrain in the vicinity of the field validation site.

In addition to the SEBS model sensitivity to T_0, the near-surface air temperature (T_a, as measured by weather stations) has a direct influence on the evaporation process and inaccuracies in measurements can lead to distorted reference ET measurements and actual ET estimates. For this reason, accuracy in air temperature measurements is needed at the weather stations themselves. Additionally, the heterogeneity of the study area (which will be described in Sect. 4.4) implies that spatially distributed air temperature across the study area is needed. This is because the spatial variations of surface characteristics (including topography and land cover) have a large influence on the near-surface weather conditions (Voogt, 2006). Increasing the accuracy of air temperature inputs will increase the likelihood of accurate ET estimates.

The sensitivity of daily ET calculated by SEBS to $\Delta(T_0 - T_a)$ for the Mouton's Valley site was modelled by varying T_0 by up to 10 K around the estimated T_0 and keeping the T_a constant. The results (Fig. 2) indicated that for the Mouton's Valley site (where the estimated T_0 is 301 K, the estimated T_a is 293 K and $(T_0 - T_a)$ equals 8 K), daily ET can vary by up to 1.5 mm in this 10 K $\Delta(T_0 - T_a)$ range. Adjusting T_a around a 10 K range, to create the same $\Delta(T_0 - T_a)$ as when T_0 was adjusted, results in a very similar daily ET range. SEBS limits evapotranspiration by setting a wet and a dry-limit. At the Mouton's Valley site, at $T_0 - T_a < 7.4$, the sensible heat flux is at the wet-limit. At the wet limit, the equation used to calculate the sensible heat flux (Eq. 6) is given in Su (2002) which differs from the sensible heat flux equations which are used when the wet-limit has not been reached (Eqs. 7, 8 and 9) (Su, 2002).

$$H_{wet} = \left((R_n - G_0) - \frac{\rho C_p}{r_{ew}} \cdot \frac{e_s - e}{\gamma}\right) \Big/ \left(1 + \frac{\Delta}{\gamma}\right) \quad (6)$$

Where e and e_s are actual and saturation vapour pressure respectively; γ is the psychrometric constant, r_{ew} is the external resistance at the wet limit and Δ is the rate of change of saturation vapour pressure with temperature.

$$u = \frac{u_*}{k}\left[\ln\left(\frac{z - d_0}{z_{0m}}\right) - \Psi_m\left(\frac{z - d_0}{L}\right) + \Psi_m\left(\frac{z_{0m}}{L}\right)\right] \quad (7)$$

$$\theta_0 - \theta_a = \frac{H}{k u_* \rho C_p}\left[\ln\left(\frac{z - d_0}{z_{0h}}\right) - \Psi_h\left(\frac{z - d_0}{L}\right) + \Psi_h\left(\frac{z_{0h}}{L}\right)\right] \quad (8)$$

$$L = \frac{\rho C_p u_*^3 \theta_v}{k g H} \quad (9)$$

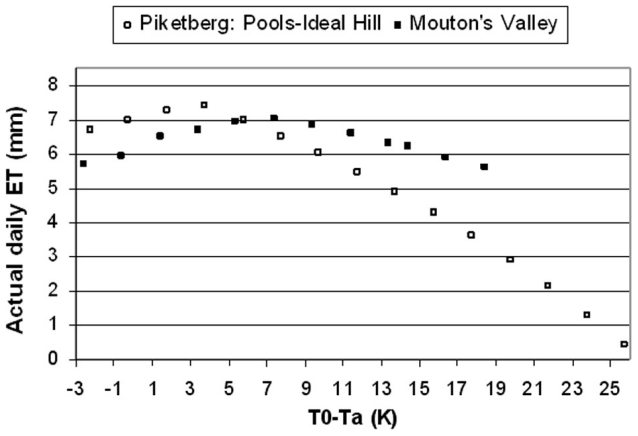

Fig. 2. Sensitivity of SEBS-estimated daily ET to $\Delta(T_0 - T_a)$ the Mouton's Valley field validation site and the Piketberg: Pools-Ideal Hill site.

where z is the height above the surface, $u*$ is the friction velocity, $k = 0.4$ is von Karman's constant, d_0 is displacement height, z_{0m} is the roughness height for momentum transfer, θ_0 is the potential temperature at the surface, θ_a is the potential air temperature at height z, z_{0h} is the scalar height for heat transfer, Ψ_m and Ψ_h are the stability correction functions for momentum and sensible heat respectively, L is the Obukhov length, g is acceleration due to gravity and θ_v is the potential virtual temperature near the surface (Su, 2002).

In Eq. (6), with decreasing $T_0 - T_a$, the denominator is decreased by the decrease in the Δ (the rate of change of saturation vapour pressure with temperature) and therefore the sensible heat flux at the wet limit increases resulting in a decrease in the latent heat flux, a decrease in the evaporative fraction and a decrease in the daily evapotranspiration. This is the reason for the decrease in daily actual evapotranspiration with $T_0 - T_a$ once the wet-limit has been reached.

Where the wet-limit has not been reached, Eqs. (7), (8) and (9) are used in the determination of the sensible heat flux. In Eq. (8), with decreasing $T_0 - T_a$, there will be decreasing sensible heat flux estimation, resulting in increasing latent heat flux and therefore increasing daily actual evapotranspiration. This explains why the daily actual evapotranspiration increases with decreasing $T_0 - T_a$ until the wet-limit is reached. At the wet-limit Eq. (6) is used and the daily evapotranspiration decreases with decreasing $T_0 - T_a$ due to decreasing saturation vapour pressure.

The modelling of the sensitivity of ET to T_0 in a dryland agriculture environment at Piketberg: Pools-Ideal Hill (where the estimated T_0 is 311 K, the measured T_a is 295 K and $T_0 - T_a$ is 16 K) is also shown in Fig. 2. It can be seen that the sensitivity of daily ET to $\Delta(T_0 - T_a)$ is greater than the Mouton's Valley site with a range of 7 mm across the same $\Delta(T_0 - T_a)$ where T_0 is increased and decreased by 10 K. In the case of the Piketberg: Pools-Ideal Hill site, the wet-limit is not reached when using similar $T_0 - T_a$ values as is used for the Mouton's Valley scenario. This is possibly due to the calculated lower roughness lengths of the Piketberg: Pools-Ideal Hill site (in combination with different atmospheric conditions) when compared with the Mouton's Valley site, resulting in a higher sensible heat flux for the same $T_0 - T_a$ as observed at the Mouton's Valley site. In the selected $T_0 - T_a$ range (10 K), the sensible heat flux is not forced to the wet limit, however when $T_0 - T_a$ is lowered further, the wet-limit drop off in evapotranspiration (which occurs at $T_0 - T_a \sim 3$ in this particular instance) is reached.

It can therefore be said that the sensitivity of daily ET to $\Delta(T_0 - T_a)$ is dependent on the land cover being studied and may also be dependent on the calculated $T_0 - T_a$ itself. It should, however, be noted that the uncertainty related to T_0 in the dryland agricultural area is almost certainly lower than the 10 K range found at the Mouton's Valley site since the dryland agricultural at Piketberg: Pools-Ideal Hill is topographically flat and relatively homogeneous. This implies that it is unrealistic to expect the extreme uncertainty in daily ET as may be implied in Fig. 2. However, it is useful to note the differences in sensitivity to $\Delta(T_0 - T_a)$ on the same day, for two land covers in close proximity to each other, therefore re-emphasizing the care that should be taken (particularly regarding the accuracy of input data) when using SEBS in a heterogeneous environment.

Furthermore, the calculated sensitivity of the sensible heat flux at the Piketberg: Pools-Ideal Hill site to $\Delta(T_0 - T_a)$ was found to be in close agreement with the sensitivity of $\Delta H = 10\Delta(T_0 - T_a)$ reported by Su (2002) for cotton, when the wet limit has not been reached. At the wet-limit, the sensitivity of the sensible heat flux to $\Delta(T_0 - T_a)$ was found to be $\Delta H = -8.32\Delta(T_0 - T_a)$. For the Mouton's Valley site, it was found that calculated sensitivity of the sensible heat flux to $\Delta(T_0 - T_a)$, is $\Delta H = -8.68\Delta(T_0 - T_a)$ where the wet limit has been reached and of $\Delta H = 6.09\Delta(T_0 - T_a)$ where the wet limit has not been reached. It can therefore be seen that the sensitivity of H (and therefore daily ET) to $\Delta(T_0 - T_a)$ is dependent on the land cover type, T_0, and whether the wet limit has been reached.

The uncertainties in the interpolation of T_a together with the uncertainties related to T_0 estimates create ambiguity with regard to the accuracy of the results. This is particularly prohibitive since these parameters are used in the initial stages of SEBS model implementation, meaning that erroneous input data would be translated through the entire processing sequence and eventually be reflected in the final calculation of actual ET.

4.2 Fractional vegetation cover

Fractional vegetation cover (fc) and its complement are used in the calculation of the roughness length for heat transfer (Su et al., 2005) which, in turn, is used in the calculation of the sensible heat flux. In addition, fc is used in the estimation of

the soil heat flux (Su, 2002) and in the preprocessing stages to assign surface emissivity values (Sobrino and El Kharraz, 2003) which are used to derive land surface temperature. Fractional vegetation cover is a user defined input into the pre-packaged version of SEBS in ILWIS and different formulations of fc are intentionally utilized in SEBS for different purposes. Therefore, the effect of the choice of formula, and its calibration, on resulting ET should be noted.

Several methods for the calculation of fc are described in the literature. These methods generally make use of leaf area index (LAI) (Choudhury, 1987, cited in French et al., 2003) as input or require pixel NDVI together with a minimum and maximum NDVI value (Carlson and Ripley, 1997; Gutman and Ignatov, 1998). These minimum and maximum NDVI values are either constant (Sobrino and El Kharraz, 2003) or can be derived directly from the scene or from a time series.

For example, if fractional vegetation cover is calculated according to the formula for vegetation proportion (Sobrino and El Kharraz, 2003):

$$\mathrm{fc} = \frac{(\mathrm{NDVI} - \mathrm{NDVI_{min}})^2}{(\mathrm{NDVI_{max}} - \mathrm{NDVI_{min}})^2} \quad (10)$$

then $\mathrm{NDVI_{min}}$ is defined to be 0.2 and $\mathrm{NDVI_{max}}$ is 0.5, where pixels with NDVI values of 0.5 or higher are considered to be fully vegetated and pixels with values of 0.2 or lower to be bare soil. The values between $\mathrm{NDVI_{min}}$ and $\mathrm{NDVI_{max}}$ represent the mixed vegetation cover with differing degrees of sparse vegetation.

In contrast with $\mathrm{NDVI_{min}}$ and $\mathrm{NDVI_{max}}$ values as defined by Sobrino and El Kharraz (2003), Fig. 3 shows the distribution of NDVI values across the entire study area for a winter wet season and summer dry season scene. It can be seen that the range of 0.2 to 0.5 is frequently exceeded within this study area, particularly in the winter wet season. The distribution of NDVI in this study area is therefore scene and season dependent.

At a NDVI value of 0.5 and higher, maximum vegetation cover is assumed and fc = 1. The assumption is therefore that the soil is completely shaded, and based on the soil heat flux equation (Su, 2002), the soil heat flux is only a function of net radiation and fractional vegetation cover, equalling 5% of net radiation. In contrast, the field validation data at TERRA overpass indicate a relatively high soil heat flux (approximately 12–16% of net radiation) since the bare soil underneath the trees receives direct radiation as a result of the solar zenith and azimuth angle in combination with the orientation of the tree rows. At AQUA overpass, when the soil of the field validation site is shaded (effectively mimicking a vegetated pixel), there is a much better agreement between field validation (approximately 3–15% of net radiation) and the SEBS results (approximately 5% of net radiation) for soil heat flux.

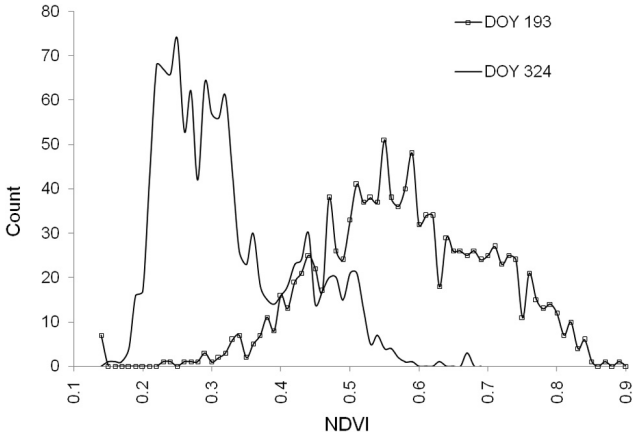

Fig. 3. NDVI distribution for the study area for a winter wet season scene (DOY 193) and a summer dry season scene (DOY 324).

The fractional vegetation cover calculation can be tested using the field validation data at Mouton's Valley and by rearranging the soil heat flux equation (Su, 2002):

$$\mathrm{fc} = -\left[\frac{\frac{G_0}{R_n} - \Gamma_c}{\Gamma_s - \Gamma_c}\right] - 1 \quad (11)$$

Where Γ_c (0.05) (Monteith, 1973 in Su, 2002) and Γ_s(0.315) (Kustas and Daughtry, 1989, in Su, 2002) are the soil heat flux ratios for full vegetation canopy and for bare soil respectively. Solving Eq. (10) by substituting the field measured G_0 values, fractional vegetation cover is calculated to range from 0.58–0.73 at TERRA overpass and at AQUA overpass from 0.67–1. If this is taken to be a true reflection of fractional vegetation cover of the apple orchard at image acquisition time, the NDVI minimum and maximum values should be adjusted as a fractional vegetation cover of 1 is not a realistic result especially at TERRA acquisition time.

Considering fc calculated above, the need for calibrating NDVI by defining an appropriate $\mathrm{NDVI_{max}}$ for the study area is apparent. Substituting this fc and the corresponding NDVI for the Mouton's Valley site for each MODIS TERRA and AQUA acquisition and keeping the $\mathrm{NDVI_{min}} = 0.2$ as suggested by Sobrino and El Kharraz (2003) in Eq. (10) results in an average $\mathrm{NDVI_{max}} = 0.65$, which is more appropriate for the study area during the field validation period.

The benefits of using a set minimum and maximum NDVI should be weighed up against using scene-specific estimates especially for scenes which do not contain a full range of vegetation cover as this will skew the results of the fractional vegetation calculation. The sensitivity of daily ET to choice of fc formula and the calibration of $\mathrm{NDVI_{min}}$ and $\mathrm{NDVI_{max}}$ is shown in Fig. 4 for the Mouton's Valley site. The curve in Fig. 4 was created by repeatedly varying fc and recomputing daily ET. The points on the curve show that for the same pixel, a different formula would produce a different fc result:

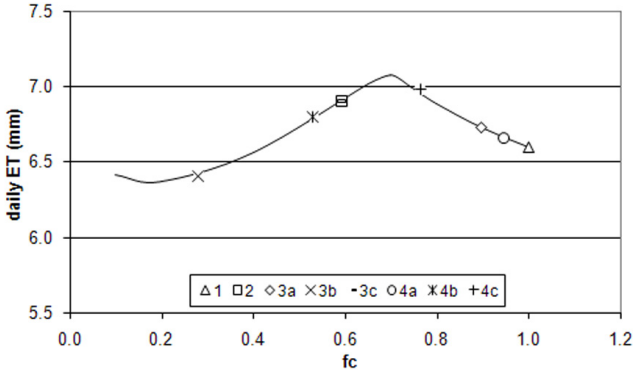

1	Fixed NDVI max (0.5) and min (0.2) (Sobrino & El Kharraz, 2003))
2	LAI dependent (Choudhury, 1987, cited in French et al., 2003)
3a	Scene dependent NDVI max (0.563) and min (0.207) (Carlson & Ripley, 1997)
3b	Time series derived NDVI max (0.863) and min (0.184) (Carlson & Ripley, 1997)
3c	Study area derived NDVI max (0.65) and min (0.2) (Carlson & Ripley, 1997)
4a	Scene dependent NDVI max (0.563) and min (0.207) (Gutman & Ignatov, 1998)
4b	Time series derived NDVI max (0.863) and min (0.184) (Gutman & Ignatov, 1998)
4c	Study area derived NDVI max (0.65) and min (0.2) (Gutman & Ignatov, 1998)
	Note: where fc is calculated to be greater than 1, then fc is taken to be equal to 1

Fig. 4. Sensitivity of SEBS-estimated ET to a range in fractional vegetation cover input values for the apple orchard field validation site. fc values resulting from specific formulae and methods are indicated.

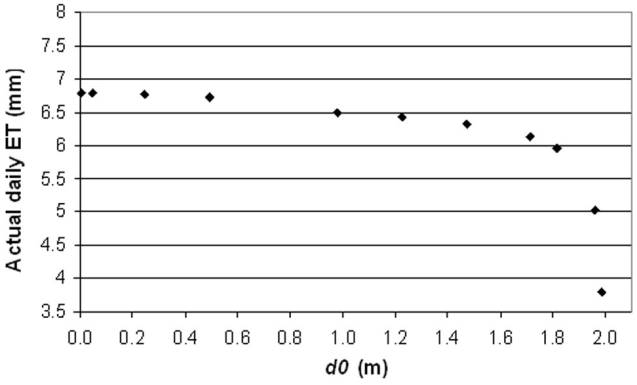

Fig. 5. Sensitivity of SEBS-estimated ET to d_0 for the Mouton's Valley field validation site when wind speed is measured at 2 m.

it can be seen that in this instance, the calculated daily ET can vary by up to 0.7 mm depending on the fc input.

From the results it can be concluded that if it is possible to obtain field data in order to derive an appropriate NDVI minimum and maximum value, the formula by Carlson and Ripley (1997) can be used. Alternatively the formula by Choudhury (1987) cited in French et al. (2003) using LAI as input may be used as it gives the same result as displayed in Fig. 4.

Fractional vegetation cover should be calculated outside of SEBS and care should be taken in the choice of formula as the variation in ET as a function of fc has been demonstrated.

4.3 Displacement height

The objective of this section is to highlight that the type of weather station and the reference height at which wind speed is measured is critical to the correct implementation of the SEBS model particularly in tall canopies.

Displacement height (d_0) values are used in combination with the reference height at which wind speed is measured (z) in the process of determining the sensible heat flux (H). d_0 can be obtained from the literature or can be empirically derived from the remote sensing vegetation inputs via the calculation of roughness length (the methodology adopted by Su, 2002; Timmermans et al., 2005; and Van der Kwast et al., 2009). Alternatively the combination approach of Jia et al. (2009) can be used. Using the empirical model, NDVI and $NDVI_{max}$ are used to determine roughness length for momentum transfer (z_{0m}) with the method described by Su and Jacobs (2001) as reported in Hailegiorgis (2006). Next, the vegetation height is calculated from z_{0m} followed by d_0 using the method of Brutsaert (1982) as reported in Hailegiorgis (2006).

In South Africa, the installation of automatic agrometeorological weather stations complies with standards set by the World Meteorological Organisation except in the height measurement of wind speed and direction. South African agrometeorological standards state that wind speed and wind direction are measured at 2 m above the surface (ARC-ISCW, 2010) in contrast to the South African Weather Service (SAWS) which measures wind speed and direction at 10 m above the surface.

A problem arises when using data from agrometeorological weather stations in canopies of 3 m or higher (where $d_0 \geq 2$), as is the case with orchards in the study area. To derive the sensible heat flux (Su, 2002) the calculation of $z - d_0$ is required, where z is the reference height at which wind speed is measured (2 m, in the case of an agrometeorological weather station). When measuring wind speed at 2 m, and solving for H using the equations defined by Su (2002) and given in Eqs. (7), (8) and (9), a situation arises where $z \leq d_0$, and the ln of a negative number needs to be solved.

In this study, the average canopy height at the Mouton's Valley site was reported to be 3.2 m in the apple orchard (Jarmain and Mengistu, 2009) and therefore $d_0 > 2$ m so the condition where $z \leq d_0$ is reached using agrometeorological weather stations. The alternative would be to use weather data from the SAWS which would allow for the sensible heat flux to be calculated for much higher canopies than for the above scenario. However, it is agrometeorological weather stations which are installed in agricultural areas where this and other studies of this nature take place. Should only agrometeorological weather station data be available, the upscaling of the available meteorological data to a higher reference height should be investigated based on radiosonde observations (Ershadi, 2010).

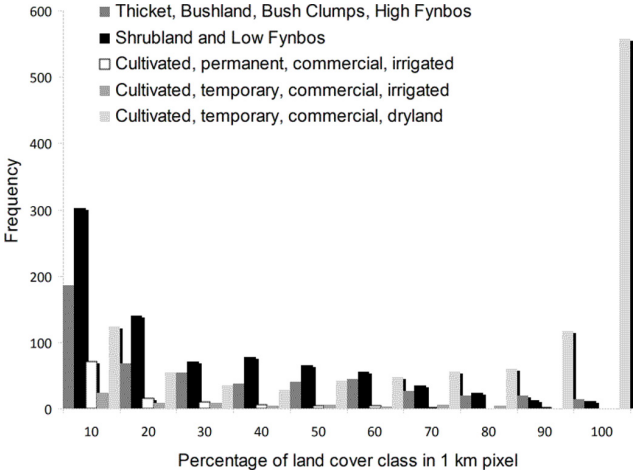

Fig. 6. Sub-pixel heterogeneity represented by the frequency with which a percentage of a particular land cover class occurs within 1 km MODIS pixels.

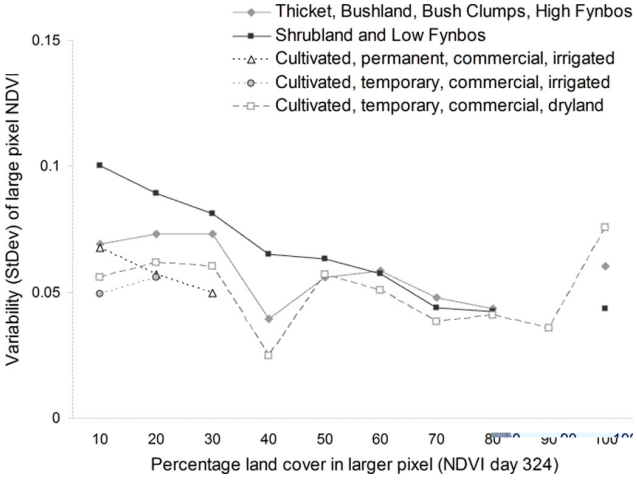

Fig. 7. Variability of NDVI within 1 km MODIS pixels in the study area, measured by standard deviation per land cover class.

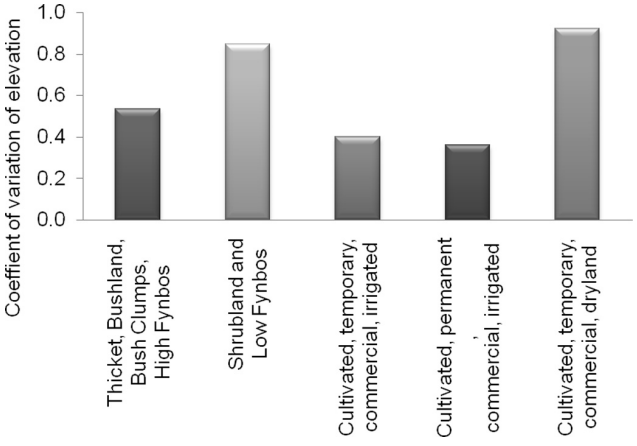

Fig. 8. Heterogeneity in topography as a function of land cover.

The effect on d_0 in high canopies is shown by using the Mouton's Valley site as an example, and testing for the sensitivity of daily ET to d_0 (Fig. 5) At approximately $d_0 = 1.8$ m, a rapid decrease in daily ET estimation is noted as d_0 approaches 2 m. It can be surmised therefore (although this should be tested in different environments and under different meteorological conditions) that when using wind speed measured at 2 m above the surface, the SEBS model should not be used in canopies of 2.7 m and higher as it is at this point that the model becomes highly sensitive to changes in d_0.

The uncertainty in the calculation of the sensible heat flux introduced when the displacement height approaches the height of wind speed measurement should be carefully considered and addressed since errors in the calculation of the sensible heat flux will be propagated through the model and will eventually influence the final ET calculation as demonstrated in this study.

4.4 Heterogeneity of the study area

Heterogeneity as related to the concept of the spatial variability of a landscape plays an important role in the application of remote sensing data to the calculation of ET, especially in the selection of the spatial resolution of the particular sensor. Various studies have shown that, for complex heterogeneous landscapes, there is lower confidence in variables derived using low resolution sensor data (Moran et al., 1997; Kustas et al., 2004; Garrigues et al., 2006; McCabe and Wood, 2006; Li et al., 2006; Li et al., 2008; Lakhankar et al., 2009) as intra-pixel spatial heterogeneity is lost due to the integration of the radiometric signal.

Land cover (mapped at 1:50 000 scale (van den Berg et al., 2008)) and topography data (elevation from SRTM at 90 m resolution) are used to demonstrate the heterogeneity of the study area. Sub-pixel variability of elevation (as a proxy for topography) and land cover are estimated within 1 km MODIS pixels in the study area. For land cover, the frequency distribution of particular land cover classes (natural and cultivated) within the 1 km pixel is used to reveal the degree of heterogeneity (Fig. 6). Figure 6 illustrates land cover heterogeneity by showing the frequency with which a particular land cover class covers a specific percentage of a 1 km MODIS pixel. For example, dryland agriculture covers up to 10% of a pixel for 124 pixels, whilst commercially irrigated agriculture covers up to 10% of a pixel for 23 pixels. Conversely, dryland agriculture covers more than 90% of a pixel for 557 pixels, whilst commercially irrigated agriculture never covers more than 80% of a pixel. Therefore, dryland agriculture is the most homogeneous land cover class with commercially irrigated classes being the most heterogeneous.

The effect of landscape heterogeneity on variables (including SEBS input parameters) derived from MODIS is illustrated using NDVI by way of example. Figure 7 shows the variability of NDVI per land cover class as measured by the standard deviation of NDVI values at 1 km resolution. The general trend shows the systematic decrease in NDVI variability as the percentage of a particular land cover in a single pixel increases. The mixed pixel effect (where more than one landcover class contributes to the spectral response of a single pixel) shown for land cover classes covering less than 40–50% can be clearly seen by the variability of the NDVI. Therefore, in more homogeneous areas, NDVI values are less variable indicating higher confidence in NDVI values and consequently, higher confidence in fractional vegetation cover estimates.

In addition to the direct effect of landscape heterogeneity and spatial resolution of input data on remote sensing variables illustrated above, landscape heterogeneity can also indirectly affect spatial modelling efforts. As an example, the topographic effects on near-surface meteorological conditions are considered. Spatial variations of surface characteristics, especially surface topography, have a large influence on the near-surface weather conditions (ARC-ISCW, 2010). The heterogeneity of the surface elevation as a proxy for variable topography can be seen from Fig. 8 which shows the coefficient of variation of elevation within each land cover class. The variation of elevation within land cover is most pronounced in the land cover classes containing dryland agriculture and low fynbos. The commercially irrigated classes show the least variability in elevation as expected since the topography is one of the variables that determines the suitability of an area for irrigated agriculture on a commercial scale.

Figure 9 illustrates the sub-pixel variation of elevation within the coarser 1 km pixel. The standard deviation increases with the mean up to elevation values of 500 m with a scattered pattern at higher elevations. The relative variability as measured by the coefficient of variation varies significantly at elevations lower than 250 m and decreases with the increase in elevation values.

The topographic variability illustrated above implies that spatially distributed measurements of near-surface weather conditions would ideally be needed for accurate retrieval of parameters needed for ET calculation, particularly in topographically heterogeneous areas. However, in the absence of distributed measurements global climate data products may be considered for catchment scale observations although these may not be suitable for field-level studies.

The effect of heterogeneity on SEBS derived ET can be illustrated by comparing the results from a single date (28 February 2008) ASTER image at 90 m resolution with the results of the same date MODIS image at 1 km resolution for the Mouton's Valley site and for the Piketberg: Pools-Ideal Hill site in Fig. 10. When the SEBS model was run on the ASTER image, it was apparent that the albedo estimation for both the homogeneous and heterogeneous sites was unrealistically low when compared with literature values. When the albedo calculation was carried out on the ASTER image which had not been atmospherically corrected, the albedo values more closely matched literature values. Since the ASTER and MODIS sensors are on board the same platform (TERRA) and the images were captured simultaneously and therefore under exactly the same atmospheric conditions with identical sensor and solar zenith angles, the SEBS model was rerun on the MODIS and ASTER data without applying atmospheric correction, in order to remove any bias that this low albedo may be introducing in the ASTER results. This approach is justified since the results are used for comparative purposes only and results are not being assessed relative to field values or images from other dates. The uncorrected images were only used in this section to analyze the impact of heterogeneity and all other results reported on in this paper are derived from images that have been atmospherically corrected.

Table 2. Heterogeneity of Mouton's Valley field validation site vs. Piketberg: Pools-Ideal Hill site illustrated by mean and standard deviation of DEM, NDVI and T_0.

	MODIS		ASTER	
Parameters	Pixel	Value	Mean	Std Dev
DEM	MV_27	641	556.98	39.67
	MV_28	641	550.87	52.26
	IH_40	187	159.14	3.56
	IH_41	179	166.57	6.48
NDVI	MV_27	0.38	0.39	0.16
	MV_28	0.38	0.45	0.16
	IH_40	0.18	0.13	0.04
	IH_41	0.16	0.11	0.01
T_0	MV_27	300.58	301.39	2.62
	MV_28	300.59	298.00	1.47
	IH_40	310.42	310.23	1.04
	IH_41	311.32	309.23	0.71

Since both the Mouton's Valley site and the Piketberg:Pools-Ideal Hill site are located close to a pixel boundary, the results of two adjacent MODIS pixels are presented and labelled MV_27 and MV_28 for the Mouton's Valley site and IH_40 and IH_41 for the Piketberg:Pools-Ideal Hill site. In Table 2 the mean and standard deviations of DEM, NDVI and T_0 at ASTER resolution (90 m) for the selected MODIS pixels at each site are shown. The standard deviations of DEM, NDVI and T_0 indicate that at ASTER resolution, the Mouton's Valley site is more heterogeneous than the Piketberg:Pools-Ideal Hill site.

Table 3. Comparison of energy partitioning in MODIS pixels for more heterogeneous Mouton's Valley field validation site: mean ASTER value per pixel vs. MODIS pixel value.

	MODIS	ASTER		Energy partitioning	
Parameter	pixel	mean	Std Dev	MODIS	ASTER
fc	0.20	0.29	0.37		
	0.20	0.43	0.41		
evaporative fraction	0.91	0.88	0.05		
	0.91	0.87	0.06		
G_0	137.30	113.96	45.99	26.20%	23.68%
	137.28	103.60	56.94	26.20%	20.26%
H	36.24	43.52	22.35	6.92%	9.05%
	36.35	53.40	30.15	6.94%	10.44%
LE	350.49	323.68	43.19	66.88%	67.27%
	350.34	354.28	36.81	66.86%	69.29%
R_n	524.03	481.17	21.90		
	523.97	511.28	18.80		
ET daily	6.38	5.72	0.36		
	6.37	5.75	0.46		

Table 4. Comparison of energy partitioning in MODIS pixel for more homogeneous Piketberg: Pools-Ideal Hill site: mean ASTER value per pixel vs. MODIS pixel value.

	MODIS	ASTER		Energy partitioning	
Parameter	pixel	mean	Std Dev	MODIS	ASTER
fc	0.00	0.00	0.00		
	0.00	0.00	0.00		
evaporative fraction	0.85	0.84	0.04		
	0.85	0.87	0.02		
G_0	121.77	106.51	5.44	31.50%	31.30%
	118.91	112.86	4.38	31.50%	31.39%
H	39.05	37.52	10.94	10.10%	11.03%
	39.25	32.73	5.70	10.40%	9.10%
LE	225.75	196.26	14.23	58.40%	57.67%
	219.34	213.91	10.25	58.10%	59.50%
Rn	386.57	340.30	15.84		
	377.50	359.50	11.38		
ET daily	6.25	5.35	0.34		
	6.09	5.71	0.26		

Tables 3 and 4 show that the R_n estimation is lower when using MODIS than when using ASTER in both the homogeneous and heterogeneous sites. In both the more heterogeneous and homogeneous area, the energy partitioning (the percentage of R_n allocated to G_0, H and LE) remains similar regardless of the resolution of the pixel. However a bigger variation in the more heterogeneous area is observed. For the Piketberg:Pools-Ideal Hill site, G_0, H and LE allocation is the same regardless of the resolution of the calculation. At the Mouton's Valley site (Table 3), the ASTER results show

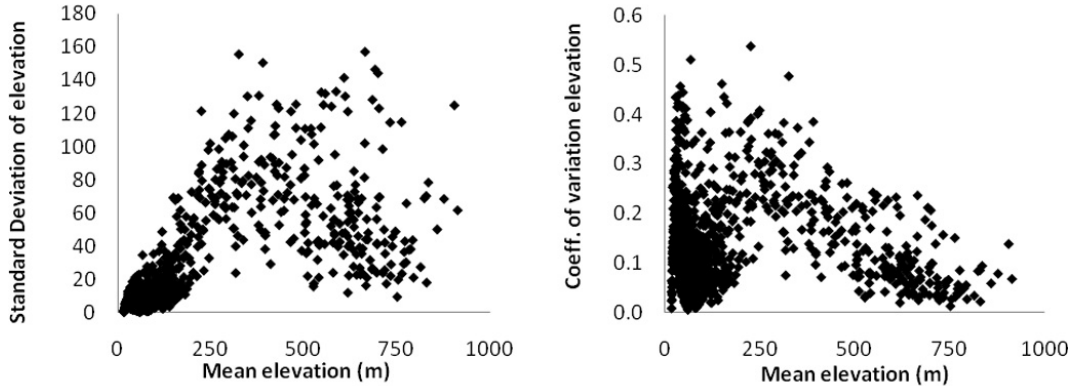

Fig. 9. Relationship of mean elevation (90 m DEM) to variability within 1 km MODIS pixels, illustrating heterogeneity of topography in the study area.

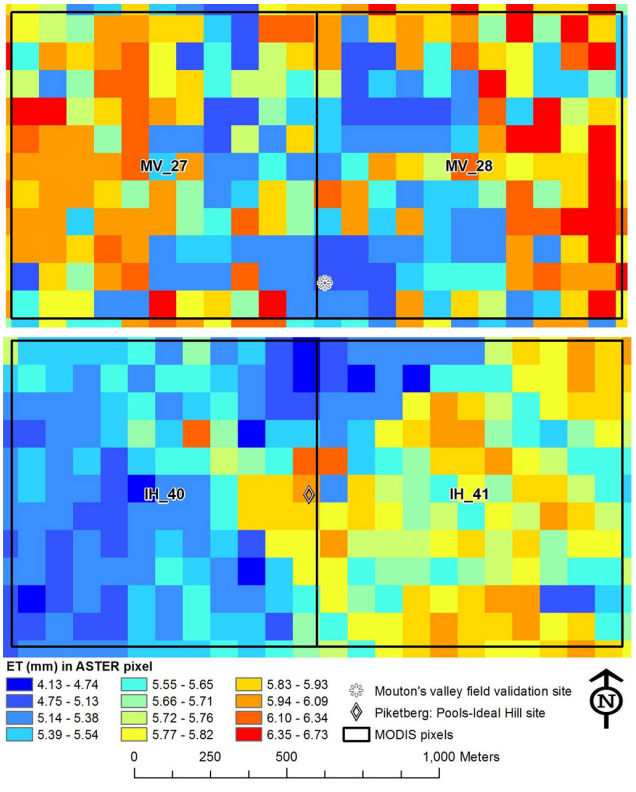

Fig. 10. SEBS derived ET from ASTER data shown in the context of two MODIS pixels for both the Mouton's Valley site (above) and the Piketberg: Pools-Ideal Hill site (below).

lower allocation of energy to G_0 and a higher allocation of energy to H when compared to the MODIS results. Energy allocation to LE is marginally higher at ASTER resolution than at MODIS resolution.

For the Piketberg:Pools-Ideal Hill site (Table 4), the ET estimated from ASTER and averaged for each of the MODIS pixels is 5.4 mm and 5.7 mm and with standard deviations of 0.34 and 0.26 for IH_40 and IH_41, respectively (Fig. 10). The ET estimated from MODIS for IH_40 and IH_41 are 6.3 mm and 6.1 mm, respectively. For the Mouton's Valley site, the ET estimated from ASTER and averaged for each of the MODIS pixel is 5.7 mm and 5.8 mm and with standard deviations of 0.36 and 0.46 for MV_27 and MV_28, respectively. The ET estimated from MODIS for both MV_27 and MV_28 is 6.4 mm. At both the more heterogeneous Mouton's Valley site and the more homogeneous Piketberg: Pools-Ideal Hill site, the ET calculated from the ASTER scene and averaged to the MODIS pixel resolution is less than the MODIS derived ET for the same pixels.

Since the difference in the evaporative fraction results (as borne out by the energy partitioning) is marginal using different pixel resolutions, it would be expected that there should be agreement between the daily ET results at both resolutions. However, since this is not the case, the difference in daily ET results can be ascribed to the upscaling of evaporative fraction to daily ET. At the heterogeneous site, even though the results from ASTER do detect more variability in the energy partitioning, the evaporative fraction results indicate that the significance of this variation is rather minimal when comparing the higher resolution results to the lower resolution results. More significant appears to be the higher daily ET results from MODIS than ASTER indicating uncertainty in the upscaling of evaporative fraction to daily ET. This suggests that, for this particular example, landscape heterogeneity is not the dominating factor at energy partitioning level whereas the resolution of the sensor does appear to play a role in the upscaling from instantaneous to daily ET through the use of albedo (Eqs. 4 and 5). Since atmospheric correction was not carried out on the images and the sample size was small, general conclusions cannot be made, although the results do point towards the importance of accurate albedo estimations for the upscaling of evaporative fraction to daily ET and that landscape heterogeneity may play a role at this level rather than at energy partitioning level.

5 Discussion

The complexities associated with the derivation of ET and the uncertainties described in Sect. 4 imply that potential errors will be introduced at various stages of ET derivation. These errors are related to error production and error propagation as defined by Veregin (1989). Error production refers to a situation where errors in output products are attributed mainly to the specific operations applied to the data, thereby producing errors in the output products while no errors were present in the original data used as input. On the other hand, error propagation refers to the process where potentially erroneous input data is passed through certain processing sequences and errors accumulate in output products. In the case of deriving ET, errors will be compounded if intermediate error-bearing output products are used in additional processing sequenced to derive the final result.

The opportunity for error production is introduced when it is considered that the SEBS model is complex in itself as it consists of three tools (Su, 2006), namely:

- a set of tools to determine physical parameters of the land surface;
- an extended model to derive roughness length for heat transfer; and
- a model to determine evaporative fraction on the basis of energy balance.

An example of error production was illustrated in the case of deriving fractional vegetation cover using ill-defined NDVI limits. An error in the calculation of fractional vegetation cover would be propagated to soil and sensible heat flux calculations. This in turn will be propagated to the calculation of the latent heat flux and therefore ET. Prior to adjusting for the study area, ET was set at the wet limit, although this was not the case after $NDVI_{max}$ was adjusted. In the absence of known suitable NDVI maximum and minimum values a priori, a fractional vegetation cover formula, such as proposed by Choudhury (1987) cited by French et al. (2003), which makes use of LAI rather than NDVI may be used.

The opportunity for error propagation is introduced at the initial stages of ET derivation when it is considered that remote sensing data together with standard meteorological data are required by the SEBS model. Due to uncertainties associated with remote sensing and the interpolation of meteorological data, potential errors will propagate throughout the processing sequence. An additional opportunity for error propagation is introduced when considering land surface temperature, air temperature and their gradient $T_0 - T_a$ since T_0 values derived from two different sources differed by up to 10 K for the field validation site. The sensitivity of SEBS to $T_0 - T_a$ appears to vary between land covers and the sensitivity may be dependent on the estimated T_0 value itself. This implies that an error in the input data would propagate through the model and cause uncertainty in the final derivation of ET. However, the range in uncertainty cannot be modelled as it appears to vary between land cover types. Furthermore, the use of air temperature from weather stations interpolated across a study area introduces more opportunities for error propagation, especially in a heterogeneous environment where T_a may vary over a short distance dependent on inter alia land cover. This will be compounded in areas with limited weather station coverage in a heterogeneous environment due to the influence of topography on near-surface weather conditions.

From the data presented here it can be seen that the study area comprises a spatially diverse landscape with a high level of heterogeneity. In order to successfully estimate ET and capture the full range of variability in fluxes, the choice of spatial resolution of remote sensing data is crucial. Kustas et al. (2004) and Li et al. (2006) found that when the spatial resolution exceeds 500 m, mixed pixels containing large contrasts in surface temperature and vegetation cover could cause significant errors (Li et al., 2008). Flores et al. (2009) also demonstrated the impact of topographic heterogeneity on near-surface soil temperature. McCabe and Wood (2006) found that MODIS has limited capacity in capturing the spatial variability in fluxes at field level but estimates for the spatial average flux at large scales may be accurate (McCabe and Wood, 2006). The results presented here differ from those reported in the listed literature in that it was found that although the absolute values for the various energy fluxes differ from MODIS to ASTER, the proportional partitioning of energy compared well between the MODIS and ASTER results at both the more homogeneous site and the more heterogeneous site. However, it is in the upscaling of evaporative fraction to daily ET where the uncertainty appears to be introduced when working at varying resolutions. The sensitivity of the SEBS model to albedo with a focus specifically on the upscaling of evaporative fraction to daily ET is lacking in the literature as often the sensitivities to input parameters are determined by assessing the sensible heat flux results (such as Badola, 2009; van der Kwast et al., 2009). Mariotto and Gutschick (2010) proposed that since most vegetation canopies are non-Lambertian reflectors, the assumption of a horizontally homogeneous Lambertian surface reflecting energy equally in all directions affects the calculations of albedo and vegetation index. They show that if the spatial variation of non-Lambertian reflectance can be formulated, the accuracy of the estimation and discrimination of ET among different land cover types can be improved. This is particularly true in a heterogeneous environment. It is possible that the assumption of Lambertian reflectance in a heterogeneous environment may be the reason for lower than anticipated albedo values at ASTER resolution.

In this paper, the sensitivities of SEBS estimated daily ET to various parameters have been shown. The sensitivities have always been related back to daily ET rather than the sensible heat flux since it is the daily ET which is of interest

to water managers and other users of the results of the SEBS model. Generalizations regarding the magnitude of errors produced by uncertainties in the input data have not been made as the dependence on study area and the interaction of various input parameters in the model was not the objective of this study. However, it has been shown that users should consider which input parameters can be calculated outside of the prepackaged version of SEBS and a decision as to which is the most appropriate methodology should be taken.

6 Concluding remarks

The results presented here can be used to improve on the project by Gibson et al. (2010) to determine the usefulness and applicability of using remote sensing technologies as a tool for resource assessment and determination of water use. Although promising, uncertainties in estimating the various parameters were encountered. These uncertainties could broadly be classified as (1) errors in input data, (2) uncertainties related to spatial heterogeneity of the study area and resolution of input data, and (3) processing errors resulting in either error production or error propagation or both.

This paper described some of these uncertainties by example of the derivation of evapotranspiration using the SEBS model. Uncertainty related to input data was demonstrated through investigating problems related to land surface and air temperature as well as in the derivation of displacement height. Uncertainty related to the heterogeneity of the study area in terms of land cover and topography in relation to the spatial resolution of input data was also demonstrated. Finally, uncertainty in data processing was demonstrated using the case of determining fractional vegetation cover as example. These uncertainties and potential errors are compounded when considering that the SEBS model for calculating ET is a complex process, requiring several image processing sequences that are combined to produce the final result. This may lead to a situation where errors may be propagated and compounded through the processing chain, eventually affecting the final output product.

The various uncertainties and potential errors of propagation and production mean that great uncertainty is associated with the accuracy of the final output product. Ideally, sources of uncertainty will need to be identified and the accumulation and propagation of errors will need to be modelled. This will enable the quantification of error or uncertainty originating either from source data or through processing errors. Simultaneous multi-parameter sensitivity analysis of inputs which are used in the SEBS model would help in determining to which parameters the SEBS model is most sensitive and under which conditions these sensitivities are the most pronounced. This would begin to address the uncertainties highlighted in this research and may lead to greater confidence in using SEBS generated ET results.

Although illustrating uncertainty using ET as an example, the derivation of all the components of the water balance equation using remote sensing data were influenced by similar uncertainties and the actual water consumption of individual agricultural fields could not be calculated. However, methodologies untested in South Africa were applied to the study area with many challenges encountered at both a data and skills capacity level. If the uncertainties and limitations encountered in the course of the research project are considered and acted upon it may be possible that at least parts of the methodology may be relevant at a later stage for water use determination.

In conclusion, users of the pre-packaged version of SEBS in Ilwis are offered the following advice: (1) Since SEBS is sensitive to the $T_0 - T_a$ gradient, care should be taken when estimating T_0 in a topographically diverse area as retrievals are less accurate in this setting. In particular, SEBS should not be used in mountainous areas with coarse resolution sensors since the heterogeneity of the T_0 cannot be captured at the appropriate scale. Furthermore, the sensitivity to $T_0 - T_a$ is also dependant on whether the wet-limit has been reached. (2) Care should be taken when selecting a fractional vegetation cover formula as this should be appropriate for the study area, especially if NDVI min and max values need to be defined. In particular, it is advised that if a LAI product is available at the appropriate scale, that it be used to estimate fractional vegetation cover according to the formula by Choudhary (1987). (3) The reference height of the weather station should be considered in relation to the canopy height of the study area. In an area where field crops with a low canopy height predominate, the use of an agrometeorological weather station is appropriate. However, where tree crops and natural vegetation with a canopy height exceeding 2.7 m are found, weather stations which measure wind speed at 10 m are probably more appropriate. (4) The scale at which the evapotranspiration results are required must be considered in relation to the choice of sensor and therefore pixel resolution and the heterogeneity of the study area. When working at a catchment scale a coarse resolution sensor may be appropriate for energy partitioning whereas, for farm or field scale results a higher pixel resolution will be required to detect inter-field or inter-farm variations. The influence of albedo on the accurate upscaling of evaporative fraction to daily ET should be considered and this may also be a function of landscape heterogeneity.

Acknowledgements. The Water Research Commission of South Africa is gratefully acknowledged for funding this research. Bob Su and Lichun Wang are gratefully acknowledged for their help and advice with the SEBS model. Eric and Michelle Stark of Mouton's Valley Farm are thanked for the use of their farm, meteorological data and allowing field experiments to be conducted on their property. Finally, the four reviewers are thanked for their very useful advice and the editor is thanked for allowing us the opportunity to improve on the original paper.

Edited by: W. Wagner

References

Alvarez, J. A. G.: Effects of land cover changes on the water balance of the Palo Verde Wetland, Costa Rica, M.Sc. thesis, International Institute for Geo-information Science and Earth Observation, The Netherlands, 2007.

ARC-ISCW: Technical manual for the AgroClimatology Weather Station Network. ARC-ISCW internal report, Agricultural Research Council-Institute for Soil, Climate and Water, South Africa, Report No. GW/A/2008/60, 2010.

Badola, A.: Validation of Surface Energy Balance System (SEBS) over forest land cover and sensitivity analysis of the model, MSc thesis, International Institute for Geo-information Science and Earth Observation, The Netherlands, 2009.

Brutsaert, W.: Evaporation into the atmosphere, Reidel, Dordrecht, The Netherlands, 299 pp., 1982.

Carlson, T. N. and Ripley, D. A.: On the relation between NDVI, Fractional Vegetation Cover, and Leaf Area Index, Remote Sens. Environ., 62, 241–252, 1997.

Choudhary, B. J.: Relationship between vegetation indices, radiation absorption, and net photosynthesis evaluated by a sensitivity analysis, Remote Sens. Environ., 22, 209–233, 1987.

Dungan, J. L., Kao, D., and Pang, A.: The uncertainty visualization problem in remote sensing analysis, in: Proceedings of Int. Geosci. Remote Se., Toronto, Canada, 2 June 2002, pp. 729–731, 2002.

Ershadi, A.: Land-atmosphere interactions from canopy to troposphere, M.Sc. thesis, International Institute for Geo-information Science and Earth Observation, The Netherlands, 2010.

Flores, A. N., Ivanov, V. Y., Entekhabi, D., and Bras, R. L.: Impact of hillslope-scale organization of topography, soil moisture, soil temperature, and vegetation on modelling surface microwave radiation emission, IEEE T. Geosci. Remote., 47, 2557–2571, 2009.

French, A. N., Schmugge, T. J., Kustas, W. P., Brubaker, K. L., and Prueger, J.: Surface energy fluxes over El Reno, Oklahoma, using high-resolution remotely sensed data, Water Resour. Res., 39, 1164, doi:10.1029/2002WR001734, 2003.

Garrigues, S., Allard, D., Baret, F., and Weiss, M.: Quantifying spatial heterogeneity at the landscape scale using variogram models, Remote Sens. Environ., 103, 81–96, 2006.

Gebreyesus, M. G.: Validation of RS approaches to model surface characteristics in hydrology: a case study in Guareña Aquifer, Salamanca, Spain, The Netherlands, MSc thesis, International Institute for Geo-information Science and Earth Observation, The Netherlands, 2009.

Gibson, L. A., Munch, Z., Engelbrecht, J., Petersen, N., and Conrad, J. E.: Remote sensing as a tool for resources assessment towards the determination of the legal compliance of surface and groundwater use, Water Research Commission, Pretoria, South Africa, WRC Report No. 1690/1/09, 2010.

Gutman, G. and Ignatov, A.: The derivation of the green vegetation fraction from NOAA/AVHRR data for use in numerical weather prediction models, Int. J. Remote Sens., 19, 1533–1543, 1998.

Hailegiorgis, W. S.: Remote sensing analysis of summer time evapotranspiration using SEBS algorithm: a case study in Regge and Dinklel, The Netherlands, M.Sc. thesis, International Institute for Geo-information Science and Earth Observation, The Netherlands, 2006.

Jarmain, C. and Mengistu, M. G.: Validating energy fluxes estimated using the surface energy balance system (SEBS) model for a small catchment, Water Research Commission, Pretoria, South Africa, Consultancy Report No. K8/824, 2009.

Jia, L., Su, Z., van den Hurk, B., Menenti, M., Moene, H. A. R., Baselga Yrisarry, J. J., Ibanez, M., and Cuesta, A.: Estimation of sensible heat flux using the Surface Energy Balance System (SEBS) and ATSR measurements, Phys. Chem. Earth, 28, 77–88, 2003.

Jia, L., Xi, G., Liu, S., Huang, C., Yan, Y., and Liu, G.: Regional estimation of daily to annual regional evapotranspiration with MODIS data in the Yellow River Delta wetland, Hydrol. Earth Syst. Sci., 13, 1775–1787, doi:10.5194/hess-13-1775-2009, 2009.

Kustas, W. P., Li, F., Jackson, T. J., Prueger, J. H., MacPherson, J. I., and Wolde, M.: Effects of remote sensing pixel resolution on modelled energy flux variability of croplands in Iowa, Remote Sens. Environ., 92, 535–547, 2004.

Lakhankar, T., Ghedira, H., Temimi, M., Azar, A. E., and Khanbilvardi, R.: Effect of land cover heterogeneity on soil moisture retrieval using active microwave remote sensing data, Remote Sensing., 1, 80–91, doi:10.3390/rs1020080, 2009.

Li, Z., Yu, G., Li, Q., Fu, Y., and Li, Y.: Effect of spatial variation on areal evapotranspiration simulation in Haibei, Tibet plateau, China, Int. J. Remote Sens., 27, 3487–3498, 2006.

Li, F., Kustas, W. P., Anderson, M. C., Prueger, J. H., and Scott, R. L.: Effect of remote sensing spatial resolution on interpreting tower-based flux observations, Remote Sens. Environ., 112, 337–349, 2008.

Liang, S.: Narrowband to broadband conversions of land surface albedo. I Algorithms, Remote Sens. Environ., 76, 213–238, 2000.

Lin, W.: Satellite based regional scale evapotranspiration in the Hebei Plain, Northeastern China, The Netherlands, M.Sc. thesis, International Institute for Geo-information Science and Earth Observation, The Netherlands, 2006.

Lin, W., van de Velde, R., and Su, Z.: Satellite based regional-scale evapotranspiration in the Hebei Plain, Northeastern China, in: Proceedings of Dragon 1: Programme Final Results 2004–2007, Beijing, 21–25 April 2008, 9 p., 2008.

Madeira, C., Dash, P., Olesen, F., and Trigo, I.: Intercomparison of Meteosat-8 derived LST with MODIS and AATSR similar products, in: Proceedings of the 2005 EUMETSAT Meteorological Satellite Conference, Dubrovnik, Croatia, 19 - 23. September 2005, available at: http://www.eumetsat.int/Home/Main/AboutEUMETSAT/Publications/ConferenceandWorkshopProceedings/2005/SP_1232458833219?l=en, 2005.

Mariotto, I. and Gutschick, V. P.: Non-Lambertian Corrected Albedo and Vegetation Index for Estimating Land Evapotranspiration in a Heterogeneous Semi-Arid Landscape, Remote Sens., 2, 926–938, 2010.

McCabe, M. F. and Wood, E. F.: Scale influences on the remote estimation of evapotranspiration using multiple satellite sensors, Remote Sens. Environ., 105, 271–285, 2006.

McCabe, M. F., Wood, E. F., Wójcik, R., Pan, M., Sheffield, J., Gao, H., and Su, H.: Hydrological consistency using multi-sensor re-

mote sensing data for water and energy cycle studies, Remote Sens. Environ., 112, 430–444, 2008.

Moran, M. S., Humes, K. S., and Pinter Jr., P. J.: The scaling characteristics of remotely-sensed variables for sparsely-vegetated heterogeneous landscapes, J. Hydrol., 190, 337–362, 1997.

Pan, M., Wood, E. F., Wójcik, R., and McCabe, M. F.: Estimation of regional terrestrial water cycle using multi-sensor remote sensing observations and data assimilation, Remote Sens. Environ., 112, 1282–1294, 2008.

Sobrino, J. A. and El Kharraz, J.: Surface temperature and water vapour retrieval from MODIS data, Int. J. Remote Sens., 24, 5161–5182, 2003.

Su, Z.: The Surface Energy Balance System (SEBS) for estimation of turbulent heat fluxes, Hydrol. Earth Syst. Sci., 6, 85–100, doi:10.5194/hess-6-85-2002, 2002.

Su, Z.: An introduction to the surface energy balance system (SEBS), Lecture notes, ESA TIGER Capacity Building Facility 1st Training Course on "Advanced optical remote sensing", Cape Town, 22–25 November 2006.

Su, Z. and Roerink, G. J. (Eds.): Drought Risk Reduction, Wageningen, Alterra, Alterra-rapport 1135, 2004.

Su, H., McCabe, M. F., and Wood, E. F.: Modeling Evapotranspiration during SMACEX: Comparing Two Approaches for Local- and Regional-Scale Prediction, J. Hydrometeorol. – Special Section, 6, 910–922, 2005.

Su, Z., Wang, L., and Parodi, G. N.: SEBS for ILWIS Open Source: A Practical Tool for Surface Energy Balance Estimates from Remote Sensing Data, Surface Energy Balance Models of Agricultural Areas from Earth Observation Data, Lima, Perú, 13 March 2008.

Timmermans, W. J., van der Kwast, J., Gieske, A. S. M., Su, Z., Olioso, A., Jia, L., and Elbers, J.: Intercomparison of energy flux models using ASTER imagery at the SPARC 2004 site, Barrax, Spain, in: Proceedings of the ESA WPP-250: SPARC final workshop, Enschede, 4–5 July 2005, 8 p., 2005.

Van den Berg, E. C., Plarre, C., Van den Berg, H. M., and Thompson, M. W.: The South African National Land Cover 2000. Agricultural Research Council-Institute for Soil, Climate and Water, Pretoria, Report GW/A/2008/86, 2008.

van der Kwast, J., Timmermans, W., Gieske, A., Su, Z., Olioso, A., Jia, L., Elbers, J., Karssenberg, D., and de Jong, S.: Evaluation of the Surface Energy Balance System (SEBS) applied to ASTER imagery with flux-measurements at the SPARC 2004 site (Barrax, Spain), Hydrol. Earth Syst. Sci., 13, 1337–1347, doi:10.5194/hess-13-1337-2009, 2009.

Veregin, H.: Error modelling for the map overlay operation, in: Accuracy of Spatial Databases, edited by: Goodchild, M. F. and Gopal, S., Taylor and Francis, London, 3–18, 1989.

Voogt, M. P.: Meteolook, a physically based regional distribution model for measured meteorological variables. M.Sc. Thesis TU Delft, abstract available at: http://www.citg.tudelft.nl/live/pagina.jsp?id=50e40a94-07c2-4ccc-a3e9-849c85ecbfd0&lang=en&binary=/doc/Voogt2006.pdf, 2006.

Wang, G., Gerther, G. Z., Fang, S., and Anderson, A. B.: A methodology for spatial uncertainty analysis of remote sensing and GIS products, Photogramm. Eng. Rem. S., 17, 1423–1432, 2005.